

Computation of the complete acoustic field with Finite-Differences algorithms

Adan Garriga, Carlos Spa and Vicente López

Departament de Tecnologia, Universitat Pompeu Fabra, Passeig de Circumval.lació 8, 08003, Barcelona (Spain)

In this paper we propose a Finite Differences scheme for the simulation of the propagation of the acoustic field, i.e. the three components of the velocity and the pressure. The scheme has been tested in simple 1D, 2D and 3D closed environments. We study in detail the computational resources needed for real-time rendering showing that the proposed integration scheme can be used in future multimedia applications.

1 Introduction

In the last decade, the new emerging multimedia technologies have forced new developments in modeling the propagation of sound waves in 3D virtual environments [1]. Historically, the first applications were in the context of the modeling of concert halls for prediction and auralization of sound [2, 3]. In the recent years new research interests have appeared driven by multimedia technological advances. Among the plethora of new applications we have to mention those derived from the entertainment industry (cinema, video games, ...); those related with music (music processing, composition and synthesis); those related with virtual environments and Virtual Reality (VR).

There are many techniques to model acoustic environments and the suitability of them depend strongly on the particular application [1]. In this paper we focus our attention in the possibility of real-time sound rendering for multimedia production. In particular, we propose a Finite Differences algorithm for the acoustic rendering in cubic rooms [4] focusing on the possibility of real-time implementation.

The paper is organized as follows: in Section 2 we define on physical grounds the acoustic problem; in Section 3 we propose an algorithm for the numerical solution of the problem; in Section 4 we make a detailed analysis of the results in one dimension while in Section 5 we show the results in two and three dimensions and finally in Section 6 we present the conclusions and the outlook of our work.

2 Statement of the Problem

Sound waves have some particularities; one of these is that they differ from waves on a string or on a membrane by being longitudinal waves. The molecules of the air move in the direction of propagation of the wave, so that there are no alternate crests and troughs (transversal waves), as with waves on the surface of water, but alternate compressions and rarefactions. The restoring force responsible for keeping the wave going is simply the opposition that the fluid exhibits against being compressed

[5]. The presence of a sound wave produces changes in density, pressure, and temperature in the fluid, each change being proportional to the amplitude of the wave. The pressure changes are usually the most easily measurable, though nowadays some sound detectors measure directly the velocity components of the air [6].

From now on, we consider the elastic case: sound waves propagate through space without loss of energy (i.e. no dissipation). The energy is only lost at the walls (boundary conditions). Then, we have to consider the classical linear equations for the acoustic field which can be written as [5],

$$\rho \frac{\partial u^x}{\partial t} + \frac{\partial P}{\partial x} = 0 \quad , \quad (1)$$

$$\rho \frac{\partial u^y}{\partial t} + \frac{\partial P}{\partial y} = 0 \quad , \quad (2)$$

$$\rho \frac{\partial u^z}{\partial t} + \frac{\partial P}{\partial z} = 0 \quad , \quad (3)$$

$$\frac{\partial P}{\partial t} + \rho c^2 \left[\frac{\partial u^x}{\partial x} + \frac{\partial u^y}{\partial y} + \frac{\partial u^z}{\partial z} \right] = 0 \quad . \quad (4)$$

Where ρ is the density of the fluid (from now on, the air) and c is the acoustic velocity inside this fluid. The velocity of the fluid is given by $\vec{u} = (u^x, u^y, u^z)$ and P is the pressure relative to a given pressure reference level (usually the atmospheric pressure). The first three equations state that a pressure gradient produces an acceleration of the fluid while the fourth states that a velocity divergence produces a compression of the fluid. These equations are valid for small velocities and small values of the relative pressure.

We have to remark that, in order to have a complete physical description of the acoustic field, it is very important to know the acoustic velocity as well as the acoustic pressure [6] and is for that reason that we work with equations (1)-(4) and not only with the wave equation for the pressure. Therefore, the numerical scheme we propose in the next section deals with the complete set of linear equations (1)-(4).

3 Finite-Differences approach

For the applications we are interested in, the acoustic spaces we shall consider consist on simple cubic rooms. There are a lot of methods for computing the acoustic field in a closed space. In general, they can be divided in two main groups: geometrical-based methods (GMs) and physical-based methods (PMs).

GMs exploit the fact that the sound field can be decomposed in elementary waves (sound field decomposition). As an example we have to mention the image source method, ray-tracing methods and more recently, beam-tracing methods [7]. These methods are very fast from a computational point of view but they lack of accuracy because a lot of approximations are taken in order to reproduce important acoustic features such as diffraction.

On the other hand, PMs deal with the exact numerical solution of the acoustic linear equations (1)-(4) ¹. These methods are very accurate in reproducing the acoustic field but are usually prohibitive from the computational resources point of view. The most common techniques used for the numerical approximation of the linear equations are Finite Differences (FD), Finite Elements (FE) and Boundary Elements (BE) methods [8].

In this paper we propose a FD algorithm in the time domain (FDTD) for the solution of equations (1)-(4). We have chosen FDTD methods by many reasons.

- FD algorithms give an accurate physical solution for the acoustic field and reproduce diffraction phenomena in a natural way.
- For animation and multimedia purposes, we have to consider cases where both the sound source and the receiver can move around. FD algorithms compute the sound field in the whole space at each time; therefore, the fact that the source or the receiver can move does not increase the computational effort.
- FDTD methods are easy to parallelize and therefore very suitable for future real-time applications.

Among all the FDTD algorithms that are in the literature we finally have chosen the MacCormack method [4] which is a two-step second order explicit method. It is well-known that in one dimension this method gives good results in accuracy for the wave equation; moreover, it is an algorithm that can be easily extended to higher dimensions and to non-linear acoustic problems.

Consider that the space is discretized on a regular grid. The nodes of the grid i at a time n are characterized by the following four quantities: velocity $\vec{u}_i^n = (u^x, u^y, u^z)_i^n$

¹Generally, only the wave equation is considered. However, new measurement devices justify the treatment of the complete set of linear equations.

and pressure P_i^n . The MacCormack method consist on integrating the equations of motion in two steps. The first step is given by:

$$(\widehat{u^x})_i^{n+1} = (u^x)_i^n - a1(P_{i+\Delta x}^n - P_i^n) , \quad (5)$$

$$(\widehat{u^y})_i^{n+1} = (u^y)_i^n - a1(P_{i+\Delta y}^n - P_i^n) , \quad (6)$$

$$(\widehat{u^z})_i^{n+1} = (u^z)_i^n - a1(P_{i+\Delta z}^n - P_i^n) , \quad (7)$$

$$\begin{aligned} \widehat{P}_i^{n+1} &= P_i^n - a2 [(u^x)_{i+\Delta x}^n - (u^x)_i^n] \\ &\quad - a2 [(u^y)_{i+\Delta y}^n - (u^y)_i^n] \\ &\quad - a2 [(u^z)_{i+\Delta z}^n - (u^z)_i^n] , \end{aligned} \quad (8)$$

where $a1 = \frac{\Delta t}{\rho \Delta x}$ and $a2 = \rho c^2 \frac{\Delta t}{\Delta x}$ are the stability constants of our problem. The second and final step is:

$$\begin{aligned} (u^x)_i^{n+1} &= \frac{1}{2} [(u^x)_i^n + (\widehat{u^x})_i^{n+1}] \\ &\quad - \frac{a1}{2} [\widehat{P}_i^{n+1} - \widehat{P}_{i-\Delta x}^{n+1}] , \end{aligned} \quad (9)$$

$$\begin{aligned} (u^y)_i^{n+1} &= \frac{1}{2} [(u^y)_i^n + (\widehat{u^y})_i^{n+1}] \\ &\quad - \frac{a1}{2} [\widehat{P}_i^{n+1} - \widehat{P}_{i-\Delta y}^{n+1}] , \end{aligned} \quad (10)$$

$$\begin{aligned} (u^z)_i^{n+1} &= \frac{1}{2} [(u^z)_i^n + (\widehat{u^z})_i^{n+1}] \\ &\quad - \frac{a1}{2} [\widehat{P}_i^{n+1} - \widehat{P}_{i-\Delta z}^{n+1}] , \end{aligned} \quad (11)$$

$$\begin{aligned} P_i^{n+1} &= \frac{1}{2} [P_i^n + \widehat{P}_i^{n+1}] \\ &\quad - \frac{a2}{2} [(\widehat{u^x})_i^{n+1} - (\widehat{u^x})_{i-\Delta x}^{n+1}] \\ &\quad - \frac{a2}{2} [(\widehat{u^y})_i^{n+1} - (\widehat{u^y})_{i-\Delta y}^{n+1}] \\ &\quad - \frac{a2}{2} [(\widehat{u^z})_i^{n+1} - (\widehat{u^z})_{i-\Delta z}^{n+1}] . \end{aligned} \quad (12)$$

This algorithm (5)-(12) is proposed as a numerical integration scheme of the linear equations of the acoustic field (1)-(4). Such a scheme has never been analyzed in full detail in this context.

In the next sections, we apply this scheme to very simple geometries in one, two and three dimensions focusing on the possibility of future real-time applications.

4 One-dimensional results

In this section we briefly review the main features of the MacCormack algorithm in one dimension. Although the

one dimensional case (one dimensional string) is not realistic it is a natural first step for analyzing carefully the features of the numerical algorithm.

As a simple test case, we have considered the propagation of an initial pressure distribution in a line of 20 meters. The density of the air is $\rho = 1.21 \text{ Kg/m}^3$ and the speed of sound considered is $c = 330 \text{ m/s}$. The initial field velocity is zero and the initial pressure distribution is an academic (non-realistic) function defined by,

$$\begin{aligned}
 P(x) &= 100(x - 8) & x \in [8, 10] \\
 P(x) &= 100(12 - x) & x \in [10, 12] \quad . \quad (13)
 \end{aligned}$$

As the initial velocity distribution is zero (the air is at rest) the initial perturbation decomposes into two waves of amplitude 100 Pa travelling in both directions. In the next sections we check the suitability of the numerical approach to reproduce the wave propagation of the initial pressure distribution (13) in different physical cases.

4.1 Boundary conditions

Let us consider the implementation of different boundary conditions. In general, we can distinguish between three different physical situations:

- **Reflecting walls:** In Figure 1 we show the evolution of the initial pressure distribution (13) with perfectly reflecting boundary conditions. The initial triangular perturbation is decomposed into two travelling waves which are reflected after hitting the corresponding wall (as can be seen in the snapshot cor-

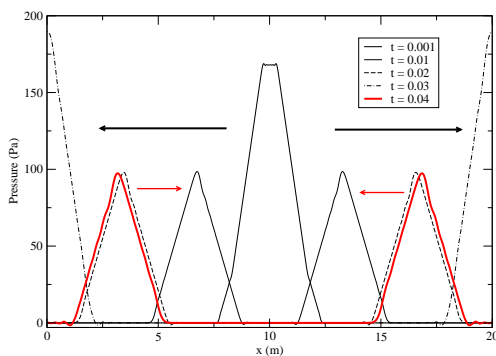


Figure 1: Time evolution of the initial distribution (13), the walls are perfectly reflecting. The wave after reflection is drawn in red.

- **Anechoic Walls:** This case corresponds to a perfectly absorbing boundary conditions. In Figure 2 we simulate the same initial pressure distribution as before. At time $t = 0.03 \text{ s}$ the energy of the waves has decreased (green line) because of the absorption

of the walls. At time $t = 0.04 \text{ s}$ the two waves have

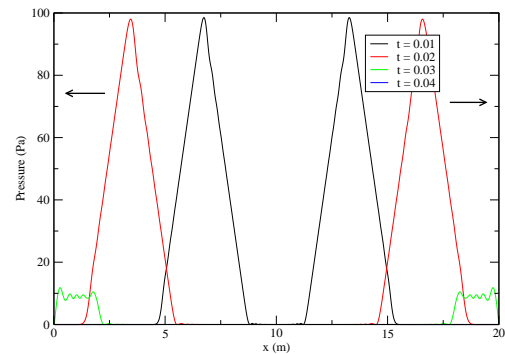


Figure 2: Plot of the evolution of the same initial perturbation. The walls are perfectly absorbing.

- **Partially absorbing walls:** Now we can consider a general wall with a given absorption coefficient. In order to implement the absorption of the wall we have defined a parameter $0 \leq \epsilon \leq 1$ in such a way that, $\epsilon = 0$ for anechoic walls while $\epsilon = 1$ for reflecting walls. In Figure 3 we can see that the left wall absorbs part of the energy of the incident wave in such a way that the amplitude of the reflecting wave is much smaller. Note that the amplitude is not reduced by a factor two, indicating that the parameter we have defined is not linear with respect to the amplitude of the incoming wave. In more general physical situations, the parameter ϵ should be frequency-dependent.

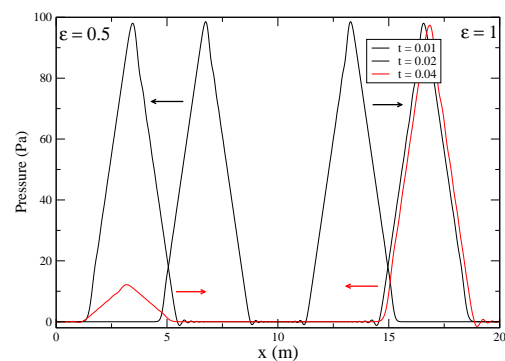


Figure 3: The same plot as before. Now, the wall located at $x = 0 \text{ m}$ has a coefficient $\epsilon = 0.5$ while the other wall is perfectly reflecting.

In these simulations the parameters we have considered are: $\Delta x = 0.02 \text{ m}$ and $\Delta t = 0.00001 \text{ s} = 0.01 \text{ ms}$. These values has been chosen in such a way that the solution is numerically stable. In the next section we will analyze with more detail the choice of the parameters.

Until now, we have considered only the propagation of a particular initial condition through space. The situation considered is not very realistic because for real applications we have to consider the propagation of sound emitted from a sound source rather than the propagation of an initial pressure distributions.

4.2 Sources

Let us consider pure sound sources in the center of the 1D room. The choice of Δx is of crucial importance depending of the pitch of the sound considered. The audible rang of frequencies is $\nu = 100 - 1500 \text{ Hz}$ which corresponds to a wavelengths λ ranging from about 20 cm to few meters. If we follow the criterion of 20 grid points per wavelength, to cover all the range we have to choose $\Delta x = 0.01 \text{ m}$. In Figure 4 we show a snapshot of the pressure distribution at a time $t = 0.01 \text{ s}$ for a periodic sound source located in the middle of the room. We show the results for three frequencies: $\nu = 100, 1000, 1500 \text{ Hz}$. In Figure 4, we have considered that the amplitude of the periodic sound signal is 2 Pa which corresponds roughly to 100 dB of Sound Pressure Level.

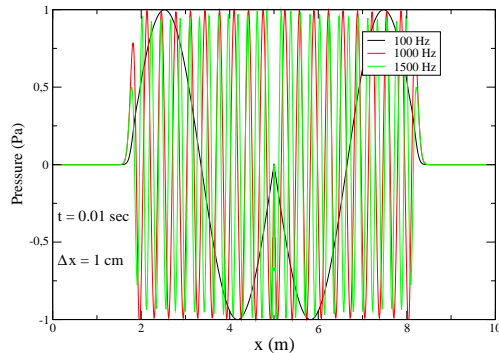


Figure 4: Three snapshots at $t = 0.01 \text{ sec}$ where there is a source in the center at frequencies $\nu = 100, 1000, 1500 \text{ Hz}$.

In this simulation we have used the following parameters: $N = 1000$, $\Delta x = 0.01 \text{ m}$ and $\Delta t = 0.00002 \text{ s}$. As can be seen in Figure 4 the results are very accurate with these parameters. Therefore, in our numerical approach we need to perform $10^5/2$ updatings for each second of the actual sound propagation. We also need 16 floating operations for updating one grid point and we have 1000 grid points. Therefore, for real-time rendering, the number of floating operations per second (FLOPS) has to be at least,

$$N_{\text{op}}^{1D} = 0.8 \text{ GFLOP},$$

which is in the range of the usual desktop computers capabilities.

4.3 Speaker/Receiver Problem

Let us consider a more realistic situation in which a Speaker S is located at $x = 2.5 \text{ m}$ of the one-dimensional room of ten meters and a Receiver R is located as an example, in $x = 7.5 \text{ m}$. In Figure 5 the speaker produces a sound which is the product of three sinusoids (black curve) and after a while, the receiver listens the audio signal (red curve) without any interference pattern (anechoic walls).

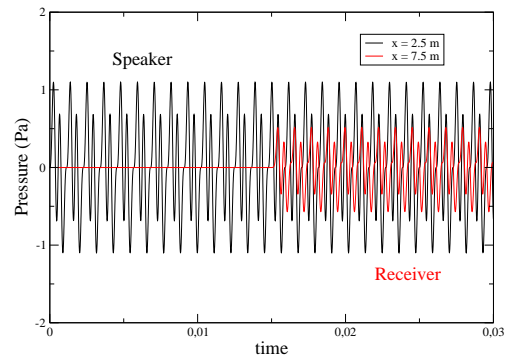


Figure 5: Sound signal pressure as a function of time for the speaker located at $x = 2.5 \text{ m}$ (black line) and for the receiver located at $x = 7.5 \text{ m}$ (red line).

The extension to more complex situations is straightforward. We only show this very simple case in order to illustrate how the algorithm works.

5 2D and 3D results.

In two dimensions the situation is pretty similar but we have to consider more grid points. As a first example, we consider a punctual sound source located at the middle of a two dimensional room. The room is 2×2 square meters. The parameters we have chosen are the same as the ones used in the one-dimensional case in order to ensure accurate results. Note that these parameters are such that the Courant number $C = c\Delta t/\Delta x$ verifies $C < 1/\sqrt{2}$ ensuring the stability of the solution in 2D [9].

In Figure 6 we show the propagation of three waves emitted with frequency $\nu = 1000 \text{ Hz}$. The algorithm reproduces exactly the wave propagation in both directions x and y . In two dimensions, the number of operations per grid point is 28 and the number of grid points is 40000. Therefore, for real-time applications, the velocity of the processor should be at least,

$$N_{\text{op}}^{2D} = 56 \text{ GFLOP},$$

which is of the order (but higher) of the power of common desktop computers.

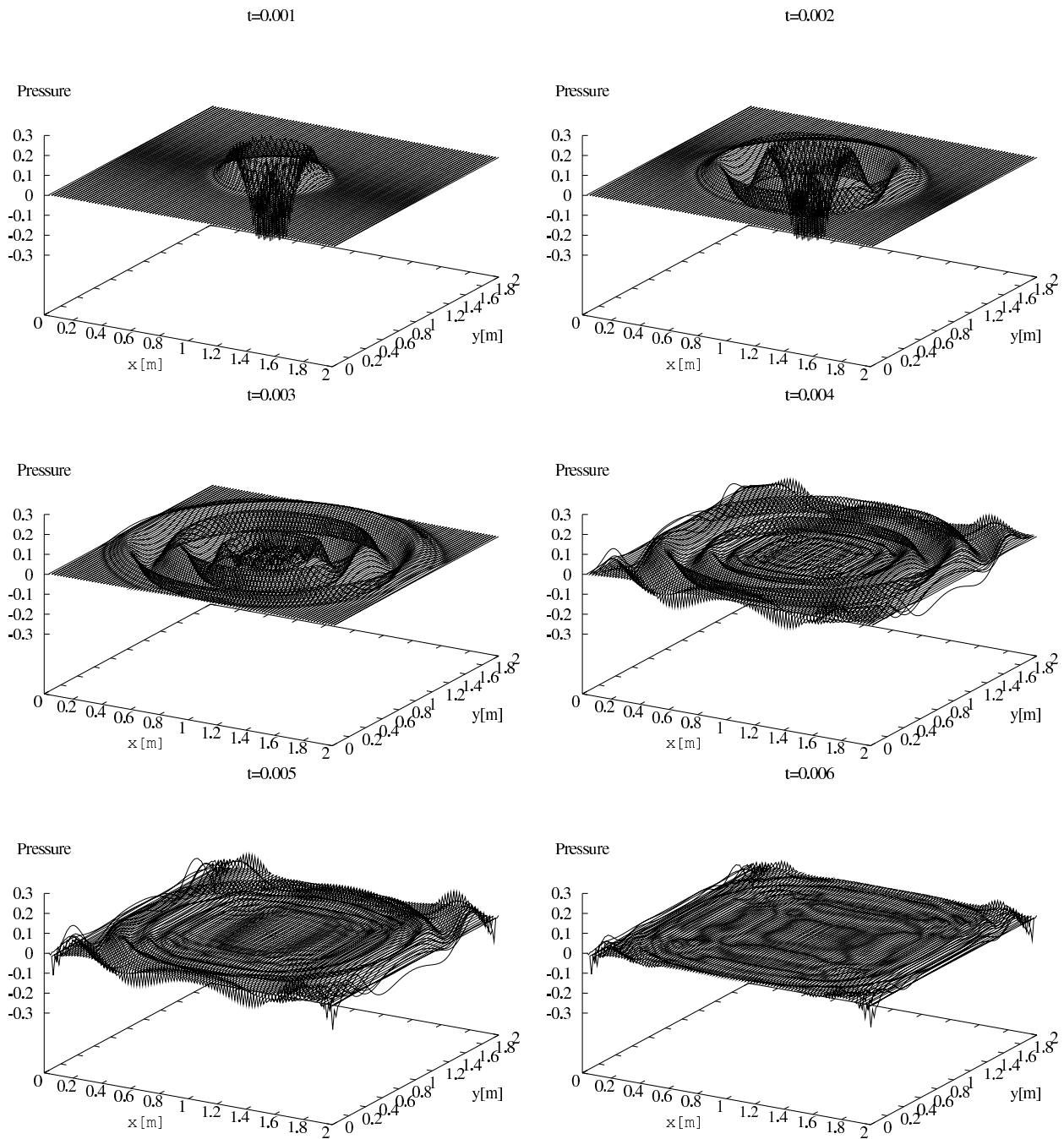


Figure 6: Six snapshots of the wave propagation of three waves emitted with frequency $\nu = 1000 \text{ Hz}$. The walls are partially reflecting $\epsilon = 0.5$. We can see how the symmetry of the propagating field changes after the collision with the walls.

In 3D we can implement the algorithm with the same quality results obtained in lower dimensions. In this case, the number of floating operations for a room of size $2 \times 2 \times 2$ is given by:

$$N_{\text{op}}^{3D} = 16 \text{ TFLOP.}$$

Note that this velocity is far away from the capabilities of desktop computers and can be only treated in real-time by supercomputers. If we want a real-time computation in 3D using a few processors, the number of grid points that can be processed in real-time with this algorithm is maybe of the order of 10^4 .

6 Conclusions

In this paper we have proposed and studied a FD explicit algorithm for computing the time propagation of the acoustic field. We have solved the four convective-like equations of the acoustic field (1)-(4) in one, two and three dimensions for a cubic rooms.

In order to test the possible applications of the algorithm we have computed the number of FLOPS needed for real-time implementation of the algorithm with high quality results. Therefore, we found an upper bound of the number of operations needed for rendering the acoustic field in simple rooms. The results can be summarized as:

$$\begin{aligned} N_{\text{op}}^{1D} &\simeq 1 \text{ GFLOP} \\ N_{\text{op}}^{2D} &\simeq 100 \text{ GFLOP} \\ N_{\text{op}}^{3D} &\simeq 10000 \text{ GFLOP.} \end{aligned}$$

In one dimension, the computations can be performed by a common desktop computer. For two dimensions we are in the limit of the capabilities of the desktop computers. Nevertheless, the algorithm we have used can be parallelized very easily and with a few processors working in parallel the acoustic field can be reproduced in real-time with high accuracy. This results will be published elsewhere.

In three dimensions the situation is more puzzling because the velocity of the processor we need for good results is of the order of TERAFLIPS. Nowadays, only supercomputers can work at this velocity.

Therefore, for 1D or 2D applications in real-time the algorithm studied is suitable in terms of accuracy and computational resources, but for 3D the applicability is restricted to non real-time applications. One of such applications we are working on is in the field of digital cinema where the acoustic field can be rendered for different scenes (i.e, different boundary conditions). Unfortunately, most of multimedia applications require 3D real-time rendering sound.

We have to stress that we have found upper bounds for the high quality rendering of acoustic fields. For real-time 3D applications, the upper bound found is beyond the capabilities of common processors and we have to try to reduce the number of FLOPS in the rendering process by introducing further approximations. One way of doing it is to combine an FDTD algorithm for low frequencies with other geometrical-based methods (GMs) for high frequencies (such as the image sources method). The fact of using GMs will introduce some inaccuracies to the acoustic field perceived by humans which for high enough frequencies should be small [10].

Acknowledgments: This work has been supported by the European Project IP-RACINE: **IST-2-511316-IP**.

References

- [1] T. Funkhouser, N. Tsingos and J-M Jot, 'Computational Sound for Graphics, Virtual Reality, and Interactive Systems'. *Course Notes N.45, SIGGRAPH 2002*, San Antonio, Texas (2002).
- [2] M.R. Schroeder and B. Atal, 'Computer simulation of sound transmission in rooms'. *IEEE Conv.Rec.* vol.11.pp. 150-155. (1963).
- [3] L. Savioja, J. Huopaniemi, T. Lokki and R. Vaananen, 'Creating interactive virtual acoustic environments'. *J. Aud. Eng. Soc.* vol.47. pp. 675-705. (1999).
- [4] J.D. Hoffman. *Numerical Methods for Engineers and Scientists*. McGraw-Hill (1992).
- [5] P.M.Morse and K.U. Ingard. *Theoretical Acoustics*. Princeton University Press (1986).
- [6] D. Stanzial and D. Bonsi, 'Evaluation of the air particle velocity signal from the binaural pressure impulse response'. *Journal of the Acoustical Society of America*, Vol. 105, Issue 2, p. 1194 (1999).
- [7] T. Funkhouser, N. Tsingos, I. Carlbom, G. Elko, M. Sondhi and J. West. 'Modeling Sound Reflection and Diffraction in Architectural Environments with Beam Tracing'. (Invited paper) Forum Acusticum, Sevilla, Spain, (2002).
- [8] T.J. Chung, 'Computational Fluid Dynamics'. Cambridge University Press, (2002).
- [9] L.R. Lines, R. Slawinski and R.P. Bording. 'A recipe for stability of finite-difference wave-equation computations'. *Geophysics*, Vol. 64, pp.967-969 (1999).
- [10] C.Spa, A. Garriga and V. López. In preparation.